JOURNAL OF SOLID STATE CHEMISTRY 82, 35–42 (1989)

Structural and Electronic Instabilities in $AgMo_6Se_8$

D. C. JOHNSON*

Chemistry Department, University of Oregon, Eugene, Oregon 97403

R. S. McLEAN

Central Research and Development Department, E. I. duPont de Nemours and Co., Inc., Experimental Station, Wilmington, Delaware 19898

AND W. R. McKINNON

Solid State Chemistry Group, Division of Chemistry, National Research Council of Canada, Ottawa, Canada K1A OR9

Received November 7, 1988; in revised form May 11, 1989

The structural parameters, superconducting critical temperatures, and magnetic susceptibilities of the solid solution $AgMo_6S_{8-x}Se_x$ are reported. The behavior of the physical properties across the solid solution are similar to those observed for other ternary molybdenum chalcogenide solid solutions, except for the end member, $AgMo_6Se_8$, which has an anomalously low superconducting critical temperature relative to those observed in the solid solution. A discontinuity in the magnetic susceptibility of $AgMo_6Se_8$ was observed at 110 K. The decrease in the Pauli susceptibility at this temperature reflects a reduction in the density of states at the Fermi level which leads to the low T_c observed for this compound. Since structural distortions are a likely cause of such anomalies, the temperature dependence of the lattice parameters of this material was investigated. A discontinuity in thermal expansion was discovered at the same temperature observed for the discontinuity in the magnetic susceptibility. This suggests that a structural distortion may be responsible for the decrease in the density of states, although our X-ray study did not show any splitting of the Bragg reflections. The presence of a structural distortion, however, also affords an explanation for the positive pressure dependence of the superconducting critical temperature of this material previously reported. The application of pressure will stabilize the high-temperature structure, thereby increasing the density of states. The increased density of states results in an increased superconducting critical temperature.

Introduction

The ternary molybdenum chalcogenides of formula MMo_6X_8 (M = Cu, Pb, La, . . .; X = S, Se, Te) exhibit a fascinating collection of physical properties: the coexistence of superconductivity with magnetic ions and magnetic ordering, extremely high critical fields, and lattice instabilities.[1] These properties have made them the subject of numerous studies since the initial report of their existence by Chevrel *et al.* in 1971 (*2*). Many of these studies have focused on the

* To whom correspondence should be addressed.

[1] For an excellent review of structural properties, see Ref. (*1a*). For physical properties, see Ref. (*1b*).

0022-4596/89 $3.00

interplay between chemical composition and physical properties, especially superconducting critical temperatures (T_c). These studies have been facilitated by the chemical flexibility of these materials.

Many of the unusual properties associated with these materials and their chemical flexibility result from their unusual structure. The structure consists of an octahedron of molybdenum surrounded by a cube of chalcogen in a manner such that each chalcogen atom caps one of the triangular faces of the octahedron. These Mo_6X_8 units then form a CsCl lattice with the ternary metal cation. The Mo_6X_8 units are rotated approximately 25° about the $\bar{3}$ axis of the cube so as to optimize the bonding distance between a general-position chalcogen atom of one cube and a molybdenum of an adjacent cube. The role of the metal cation in these structures is mainly to provide electron density to the molybdenum cluster (*3*). The metal cations, however, also effect the intercluster orientation of the Mo_6X_8 units. A more complete discussion of the structure and the effect of the metal cations upon the structure can be found in the many review articles on these materials (*1*).

Among the collection of unusual properties found in these compounds are the presence of lattice distortions as a function of temperature. These distortions are of two major types: a disorder–order transition of the ternary metal cation when more than one such cation can be present in the structure such as found in $Cu_xMo_6X_8$ (*3*) and a distortion of the metal octahedron found in MMo_6X_8 phases, typified by the $M^{2+}Mo_6S_8$ compounds (*4–7*). Both types of structural distortions typically result in a change in the thermal expansion coefficients and/or volume, with the low-temperature phase generally having a small expansion coefficient and a larger volume (*8*). These physical distortions described above lead to a reduction in the density of states at the Fermi level due to a lowering of symmetry. The reduction in the density of states can be observed as a drop in the magnitude of the Pauli paramagnetism of the conduction electrons (*7*).

In the BCS theory (*9*) the superconducting critical temperature is given by

$$T_c = \langle\omega\rangle \exp(-1/NV), \qquad (1)$$

where $\langle\omega\rangle$, the mean phonon frequency, measures the stiffness of the lattice; N measures the density of states at the Fermi level (equivalent to the number of canonical forms of equal energy in resonance); and V measures the electron–phonon coupling constant. The presence of these lattice instabilities results in the lowering of the T_c of these materials due to the reduction in the density of states. Changes in the phonon spectrum and the electron phonon coupling constant as a result of the distortion also contribute to the observed T_c, but are much more difficult to quantify (*7*).

Since the change in volume as a function of temperature is altered as a result of the distortions, the application of pressure will affect the energetics of the distortion. The application of pressure will favor the lower volume structure. For the ternary molybdenum chalcogenides, the application of pressure generally favors the high-temperature structure since it would have a lower volume than the distorted phase (*10*). Since the depression of the distortion raises the density of states at the Fermi level, the superconducting critical temperature is observed to increase as a function of increasing pressure as shown by Shelton, Chu, and others for ternary molybdenum chalcogenides with lattice instabilities (*10–12*).

In this paper, we explore the physical properties of the $AgMo_6Se_xS_{8-x}$ solid solution. This system was chosen as a result of a study by Shelton (*10*), which reported an increase in T_c as a result of pressure in $AgMo_6Se_8$. Our aim was to find evidence for a structural distortion resulting in a decrease in the density of states for $AgMo_6Se_8$

and explore how this feature evolves across the solid solution.

Experimental Section

Sample preparation. The $AgMo_6Se_xS_{8-x}$ solid solution was prepared from ultrapure starting elements. Appropriate amounts of the elements to form 1-g samples were placed in previously degassed silica tubes, which were degassed again at 10^{-6} Torr and sealed. All the tubes were placed together in a box furnace and the temperature was slowly raised to 1050°C over the course of 5 days. After 24 hr at 1050°C, the samples were cooled in air and vigorously shaken so as to homogenize. They were immediately reheated to 1100°C, kept there for 48 hr, and then air cooled. The samples were opened in a helium Dri-lab and thoroughly ground. After sealing in new degassed silica ampules, the samples were heated at 1220°C for 96 hr and finally air-cooled.

Powder X-ray diffraction. X-ray diffraction photographs were made using a 114.6-mm-diameter Debye–Scherrer camera with nickel-filtered Cu$K\alpha$ radiation. The films were read with a computer-automated densitometer and the line positions were corrected for film-shrinkage. Lines were indexed with the aid of a Fortran program that calculated the positions and intensities of possible reflections from single-crystal data (*1*). A least-squares fit, with corrections for absorption and camera-radius error, was performed with all lines with $\theta(hkl) > 30°$ that could be indexed unambiguously. The procedure yields lattice parameters with errors of less than 1 part per thousand.

Superconducting transition determination. The transition to the superconducting state was monitored by using an ac mutual-inductance apparatus, similar to one which has been described elsewhere (*13*). In this device, the detection system is a primary coil with two opposed secondary coils wound symmetrically about it. The sample was placed in one of the secondary coils, and onset of superconductivity was signaled by an imbalance between the secondary coils due to an abrupt increase in magnetic shielding that occurred when the sample became perfectly diamagnetic. Temperature was measured with a calibrated silicon diode, which was checked against the transition temperatures of lead, tin, and niobium. The T_c value was taken as the temperature at which the inductively measured transition was half-complete. The width of the transition was defined as the temperature difference between the points where the transition is 10 and 90% complete.

Magnetic susceptibility. Magnetic susceptibilities were measured from 1.8 K (or T_c) to room temperature by the Faraday technique with the use of an apparatus similar to one described previously (*14*). The balance was calibrated by using $HgCo(SCN)_4$ as a standard. Samples were held in Spectrosil quartz buckets. All samples were run over a range of fields (5–22.5 kG); susceptibilities were found to be field independent. The reported susceptibilities have been corrected for the susceptibility of the quartz buckets.

Variable temperature X-ray diffraction. X-ray diffraction patterns were obtained as a function of temperature using an automated diffractometer with nickel-filtered Cu$K\alpha$ radiation. The temperature of the sample was controlled using a Displex cryostat which sits on top of the diffractometer. The sample itself is attached to a cold finger and is enclosed within a beryllium can. The main limitation of this system is the change in the thermal expansion of the finger as a function of temperature which causes the sample to move relative to the diffractometer axis, causing an off-axis shift of the sample. We have corrected for this movement by refining the Bragg peaks

TABLE I

CRYSTAL DATA FOR THE $AgMo_6S_{8-x}Se_x$ SOLID SOLUTION

Composition x	Hexagonal parameters			Rhombohedral parameters		
	a_h (Å)	c_h (Å)	c_h/a_h	a_r (Å)	α_r (deg)	V_r (Å^3)
0.00	9.315(1)	10.848(2)	1.1645(4)	6.481(1)	91.89(7)	271.7(1)
0.80	9.353(2)	10.889(1)	1.1642(4)	6.507(1)	91.90(9)	275.0(2)
1.60	9.392(2)	10.930(2)	1.1638(5)	6.532(2)	91.92(9)	278.3(2)
2.40	9.434(2)	10.966(2)	1.1624(4)	6.560(1)	91.96(10)	281.8(2)
3.20	9.479(2)	11.006(2)	1.1611(5)	6.589(1)	92.00(10)	285.5(2)
4.00	9.511(2)	11.043(2)	1.1611(5)	6.611(1)	92.00(11)	288.4(2)
4.80	9.548(2)	11.089(2)	1.1614(4)	6.637(1)	91.99(10)	291.8(2)
5.60	9.582(3)	11.145(3)	1.1631(6)	6.664(1)	91.94(13)	295.4(2)
6.40	9.612(3)	11.184(2)	1.1635(5)	6.685(2)	91.93(13)	298.3(2)
8.00	9.671(2)	11.312(3)	1.1697(5)	6.738(2)	91.73(12)	305.5(2)

both for the lattice parameters and for the shift.

Results and Discussion

The powder X-ray diffraction patterns indicated that the compounds were pure with respect to X-ray analysis. The lone exceptions to this were found in the selenium end of the solid solution in which $MoSe_2$ was observed as a trace (less than 5%) impurity in $AgMo_6Se_8$. The amount of $MoSe_2$ was not significantly reduced through repeated annealing. The ampoule containing $AgMo_6Se_{7.2}S_{0.8}$ cracked during the last heating cycle and was not used in this study.

The lattice parameters of the $AgMo_6Se_xS_{8-x}$ solid solution are given in Table I. This solid solution follow Vegards Law, in that the unit cell volume is linear with composition on selenium for sulfur replacement. As discussed previously, the variation in the hexagonal lattice parameters with composition implies a slight preference of sulfur for the special position sites, but this ordering is very weak when compared to that observed in the La $Mo_6Se_xS_{8-x}$ solid solution (*15*).

The superconducting critical temperatures are plotted as a function of temperature in Fig. 1. The transition temperatures drop rapidly from a high of 7.73 K observed for $AgMo_6S_8$ to a minimum of 3.9 K observed in the middle of the solid solution. The superconducting temperature begins to rise as more selenium is added before finally dropping again for the pure selenide. This behavior is atypical of solid solutions of the ternary molybdenum chalcogenides in which the transition temperatures usually follow a parabolic curve across the solid solution with the end members having the highest T_c or the superconducting critical temperature drops continuously across the solid solution. The drop in T_c across a solid solution is usually attributed to the disorder caused by the random substitution in the solid solution (*16–18*). The low T_c with respect to the mixed chalcogenides in the solid solution observed for the selenium compound suggests that another mechanism is responsible for its anomalously low T_c. The magnetic susceptibilities of the various members of the solid solution were measured in our search to explain the unusual composition dependence of the superconducting critical temperature.

The temperature dependence observed in the magnetic susceptibilities of all the samples are very similar except for that of

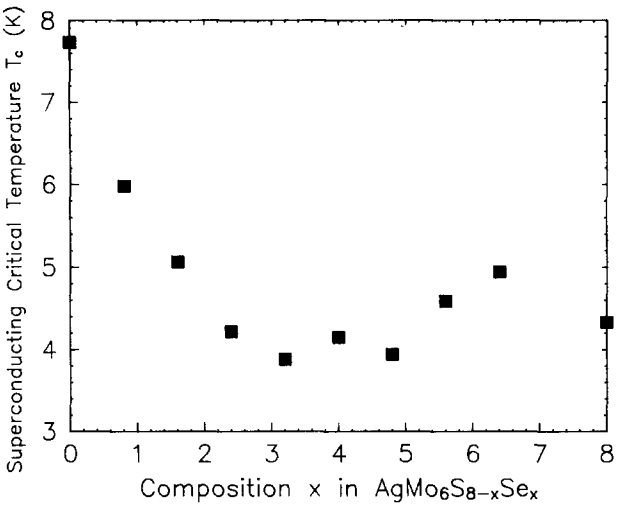

FIG. 1. The composition dependence of the superconducting critical temperature for the $AgMo_6S_{8-x}Se_x$ solid solution.

$AgMo_6Se_8$. The susceptibilities were found to be field independent. All of the samples show a very small Curie-like tail at the lowest temperatures. As the temperature is increased, the susceptibility also increases in an approximately linear manner over the temperature range measured. The data can be fit to

$$\chi_m(\text{obs}) = C_m/T + BT + \chi_m(0\ K), \quad (2)$$

where C_m is the Curie constant, B is the linear slope in the data, and $\chi_m(0\ K)$ is the susceptibility extrapolating to 0 K. This term results from the Pauli paramagnetism of the conduction electrons (the observed susceptibility has been corrected for the diamagnetism of the core electrons). The Curie constants ($\sim 1 \times 10^{-4}$ emu K) are indicative of a small amount (several parts per million) of a paramagnetic impurity. These impurities were likely to have been introduced during the repeated heating and grinding cycle used to synthesize these materials as the amount of impurities were found to increase with repeated annealing. There is a qualitative correlation between the temperature dependence of the susceptibility and the superconducting critical temperature. As the slope increases, T_c also increases. Table II summarizes the results of the fits to Eq. 2 for each of the samples measured.

TABLE II

PARAMETERS OBTAINED BY FITTING THE MOLAR MAGNETIC SUSCEPTIBILITY AS A FUNCTION OF TEMPERATURE TO THE EQUATION $\chi_m(\text{obs}) = C_m/T + BT + \chi_m(0\ K)$ FOR THE $AgMo_6S_{8-x}Se_x$ SOLID SOLUTION

Composition x	Curie constant C_m (emu K/mole $\times 10^6$)	Slope B (emu/K mole $\times 10^6$)	Pauli susceptibility $\chi_m(0\ K)$ (emu/mole $\times 10^6$)
0.00	1430	0.66	36
0.80	588	0.58	100
1.60	534	0.51	139
2.40	261	0.16	264
3.20	841	0.26	231
4.00	590	0.29	191
4.80	1270	0.16	204
5.60	560	0.42	217
6.40	1328	0.42	234

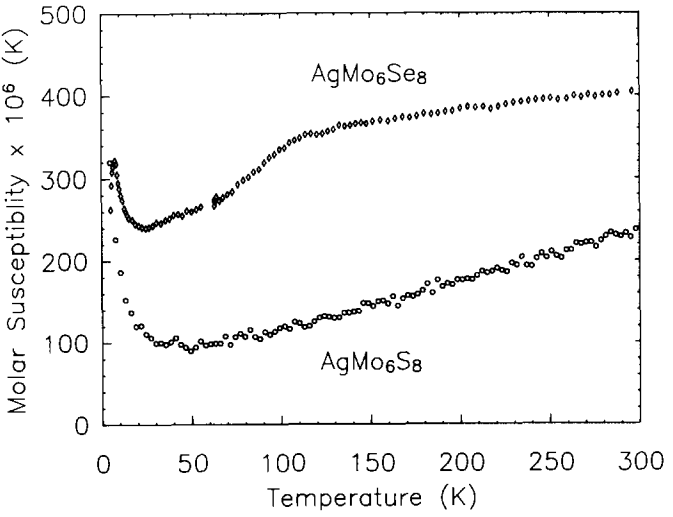

FIG. 2. The molar susceptibility of $AgMo_6S_8$ and $AgMo_6Se_8$ as a function of temperature.

The observed temperature dependences are not characteristic of simple metallic systems in which the Pauli paramagnetism is usually temperature independent. The linear slope of the magnetic susceptibility has also been observed in other ternary molybdenum chalcogenide systems and also in some of the A-15 compounds. This behavior has been attributed either to structure in the density of states or to the correlation of the electrons as a result of electron–phonon interactions (*19*).

The magnetic susceptibilities of $AgMo_6S_8$ and $AgMo_6Se_8$ are contrasted in Fig. 2. The susceptibility of $AgMo_6S_8$ drops smoothly and continuously as a function of temperature. The susceptibility of $AgMo_6Se_8$ drops slowly as the temperature is reduced until 100 K. At this point there is a discontinuity in the susceptibility as the susceptibility drops much faster as the temperature is further reduced. The most likely cause of this discontinuity is a structural distortion which results in a decrease in the density of states. Examples of structural distortions causing such a drop in the density of states are charge density waves as found in the transition metal dichalcogenides and lattice distortions as observed in $PbMo_6S_8$ and other ternary molybdenum chalcogenides (*3–7*). We measured the structural lattice parameters as a function of temperature in an attempt to find evidence for a structural distortion.

Careful diffraction patterns were collected both above and below 100 K in an attempt to observe new Bragg peaks and/or splitting of the old ones. No new peaks and no splitting of the old ones were observed. A similar situation was observed for several other ternary molybdenum chalcogenides which were latter shown to have lattice distortions. Shevchenko *et al.* (*20*) investigated the low-temperature diffraction patterns of a sintered $PbMo_6S_8$ sample and observed no splitting of diffraction peaks. Baillif *et al.* (*5*) studied the low-temperature X-ray powder diffraction patterns of sintered samples of $EuMo_6S_8$ and $BaMo_6S_8$ and observed only line broadening while for more crystalline samples prepared from melts the low-temperature X-ray lines broadened and split as the temperature was lowered.

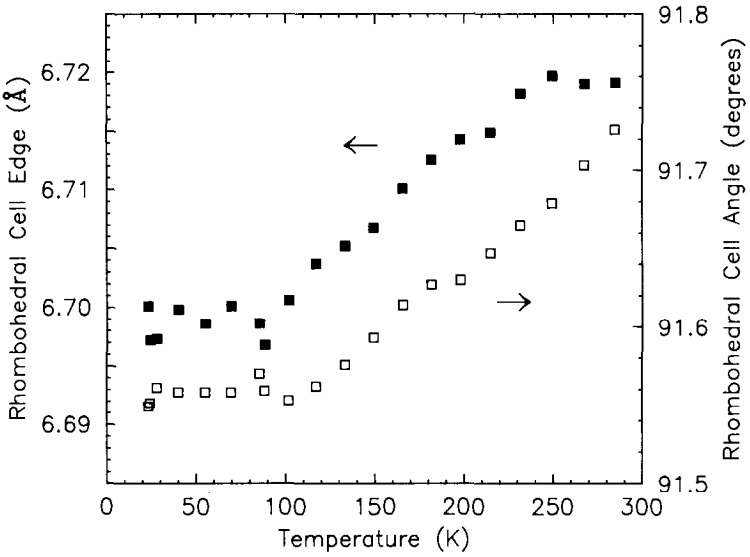

FIG. 3. The variation of the rhombohedral lattice parameters of $AgMo_6Se_8$ as a function of temperature.

The lattice parameters obtained from these studies for $AgMo_6Se_8$ are plotted as a function of temperature in Fig. 3. It is clear that there is a discontinuity in the thermal expansion at 100 K. A similar discontinuity was observed in the thermal expansion of $PbMo_6S_8$ (*21*). Later neutron diffraction studies on $PbMo_6S_8$ confirmed that this discontinuity is the result of a structural distortion (*22*). In view of these previous studies, the anomaly in the thermal expansion of $AgMo_6Se_8$ is most likely also due to a structural distortion, which is too small to be resolved by our instrumentation.

In light of the findings of this study, the opposite pressure dependences of the superconducting transition temperatures observed for $AgMo_6S_8$ and $AgMo_6Se_8$ can be explained. For $AgMo_6S_8$, we observed no anomalies in its physical properties which agrees with the observed decrease in the T_c with pressure. For $AgMo_6Se_8$, however, we have found evidence for a structural and/or electronic instability at 100 K. This instability is apparent as the observed discontinuity in the magnetic susceptibility and as the discontinuity in the temperature dependence of the thermal expansion. The application of pressure to $AgMo_6Se_8$ will favor the high-temperature phase since it has a larger thermal expansion coefficient than the low-temperature phase. The high-temperature phase also has a higher density of states as deduced from our magnetic susceptibility results. Therefore, the application of pressure increases the density of states over that found for the phase in the absence of pressure and therefore increases the superconducting critical temperature.

Acknowledgments

Acknowledgment is made to the Office of Naval Research Grant No. 87-K-0543 and to the Donors of The Petroleum Research Fund, administered by the American Chemical Society, for partial support of this research.

References

1. (*a*) K. YVON, *Curr. Top. Mater. Sci.*, 3 (1979); (*b*) O. FISCHER, *Appl. Phys.* **16,** 1 (1978).
2. R. CHEVREL, M. SERGENT, AND J. PRIGENT, *J. Solid State Chem.* **3,** 515 (1971).

3. K. YVON, A. PAOLI, R. FLUKIGER, AND R. CHEVREL, *Acta Crystallogr., Sect. B* **33,** 3066 (1977).
4. R. BAILLIF, A. JUNOD, B. LACHAL, J. MULLER, AND K. YVON, *Solid State Commun.* **40,** 603 (1981).
5. R. BAILLIF, A. DUNAND, J. MULLER, AND K. YVON, *Phys. Rev. Lett.* **47,** 672 (1981).
6. B. LACHAL, R. BAILLIF, A. JUNOD, AND J. MULLER, *Solid State Commun.* **45,** 849 (1983).
7. D. C. JOHNSON, J. M. TARASCON, AND M. J. SIENKO, *Inorg. Chem.* **24,** 2598 (1985).
8. A. W. WEBB AND R. N. SHELTON, *J. Phys. F* **8,** 261 (1981).
9. J. BARDEEN, L. N. COOPER, AND J. R. SCHRIEFFER, *Phys. Rev.* **106,** 162 (1957); **108,** 1175 (1957).
10. R. N. SHELTON, *in* "Superconductivity in d and f Band Metals" (D. H. Douglass, Ed.), pp. 137–160. Plenum, New York (1977).
11. C. W. CHU, S. Z. HAUNG, C. H. LIN, R. L. MENG, AND M. K. WU, *Phys. Rev. Lett.* **46,** 276 (1981).
12. D. W. HARRISON, K. C. LIM, J. D. THOMPSON, C. Y. HAUNG, P. D. HAMBOURGER, AND H. L. LUO, *Phys. Rev. Lett.* **46,** 280 (1981).
13. W. G. FISHER, Ph.D. Thesis, Cornell University (1978).
14. D. C. JOHNSON, Ph.D. Thesis, Cornell University (1983).
15. D. C. JOHNSON, J. M. TARASCON, AND M. J. SIENKO, *Inorg. Chem.* **22,** 3773 (1983).
16. R. CHEVREL, M. SERGENT, AND O. FISCHER, *Mater. Res. Bull.* **10,** 1169 (1975).
17. J. M. TARASCON, D. C. JOHNSON, AND M. J. SIENKO, *Inorg. Chem.* **21,** 1505 (1982).
18. J. M. TARASCON, F. J. DISALVO, J. V. WASZCZAK, AND G. W. HULL, JR., *Phys. Rev. B* **31,** 1012 (1985).
19. F. S. DELK AND M. J. SIENKO, *Inorg. Chem.* **19,** 1352 (1980).
20. A. D. SHEVCHENKO, O. V. ALEKSANDROV, S. V. DROZDOVA, G. A. KALYUZHNAYA, K. V. KEISELEVA, V. F. SHEVCHYK, AND V. E. YACHNEMEV, *Sov. J. Low Temp. Phys. (Engl. Transl.)* **8**(7), 342 (1982).
21. M. MAREZIO, P. D. DERNIER, J. P. REMEIKA, E. CORENZWIT, AND B. T. MATTHIAS, *Mater. Res. Bull.* **8,** 657 (1973).
22. J. D. JORGENSEN AND D. G. HINKS, *Solid State Commun.* **53,** 289 (1985).